**IMECE2004-62188**

# TACKLING THE TRANSITION: A MULTI-MODE COMBUSTION MODEL OF SI AND HCCI FOR MODE TRANSITION CONTROL

**Matthew J. Roelle**
Design Group
Dept. of Mechanical Engineering
Stanford University
Stanford, California 94305
Email: roelle@stanford.edu

**Gregory M. Shaver**
Design Group
Dept. of Mechanical Engineering
Stanford University
Stanford, California 94305
Email: shaver@stanford.edu

**J. Christian Gerdes**
Design Group
Dept. of Mechanical Engineering
Stanford University
Stanford, California 94305
Email: gerdes@stanford.edu

## ABSTRACT

Homogeneous charge compression ignition (HCCI) offers a promising way to improve efficiency and emissions. However, when HCCI is induced by reinducting exhaust gases, less power is produced. A possible solution is to couple HCCI with spark ignition (SI) operation at higher loads. This requires a way to smoothly switch between combustion modes. The authors present a multi-cycle, multi-mode combustion model to aid in understanding and controlling the mode transition. The model captures early ignition and low work after a switch from SI to HCCI. Furthermore, the model reveals a need to coordinate intake and exhaust valve timing to correct the HCCI phase and work. To demonstrate the model, the paper concludes with an example trajectory that maintains constant work and ignition phasing after a switch from SI to HCCI.

## NOMENCLATURE

$A_k$    Arrhenius rate pre-exponential factor
$A_e$    Surface area of exhaust manifold
$A_{ev}$    Area of exhaust valve
$A_{iv}$    Area of intake valve
$a_k$    Arrhenius rate propane concentration exponent
$A_c$    Exposed cylinder surface area
$a_W$    Wiebe constant
$B_c$    Cylinder bore diameter
$b_k$    Arrhenius rate oxygen concentration exponent
$\hat{c}_p$    Molar specific heat

$C_D$    Coefficient of discharge
$E_k$    Arrhenius rate activation energy
EVC    Exhaust valve closing time
EVO    Exhaust valve opening time
$\gamma$    Specific heat ratio
$h$    Enthalpy
$\hat{h}$    Molar enthalpy
$\bar{h}$    Convection coefficient
IVC    Intake valve closing time
IVO    Intake valve opening time
$M$    Molecular mass
$m$    Mass
$\dot{m}$    Mass flow rate
$m_W$    Wiebe constant
$N$    Number of moles
$n_k$    Arrhenius rate temperature exponent
$\omega$    Engine speed of rotation
$p$    Pressure
$\phi$    Equivalence ratio, $\frac{(fuel/air)}{(fuel/air)_{stoich}}$
$Q$    Heat transfer
$R$    Specific gas constant
$\hat{R}$    Molar universal gas constant
$\Psi$    Integrated global Arrhenius rate
$\Psi_{th}$    Integrated global Arrhenius rate threshold
$T$    Temperature
$\theta$    Engine position
$\Delta\theta$    Wiebe function combustion duration
$u$    Internal energy

| | |
|---|---|
| $V$ | Volume |
| $\bar{v}_p$ | Mean piston velocity |
| $W$ | Work |
| $[X]$ | Species concentration in terms of moles per unit volume |
| $Y$ | Mass fraction |
| $a$ | Subscript denoting an ambient parameter |
| $i$ | Subscript denoting an intake parameter |
| $c$ | Subscript denoting a cylinder parameter |
| $e$ | Subscript denoting an exhaust parameter |
| $j$ | Subscript denoting a species enumeration |
| $ign$ | Subscript denoting an ignition parameter |
| $ic$ | Subscript denoting flow from intake to cylinder |
| $ce$ | Subscript denoting flow from cylinder to exhaust |
| $ec$ | Subscript denoting flow from exhaust to cylinder |
| $ea$ | Subscript denoting flow from exhaust to ambient |
| $rxn$ | Subscript denoting a reaction parameter |

## INTRODUCTION

As automotive engine designers pursue methods of improving engine efficiency, emissions and performance, multiple-combustion-mode engines open a new realm of possibilities. A multi-mode engine coupling spark ignition (SI) with homogeneous charge compression ignition (HCCI) could have the range and startability of SI and the efficiency and low $NO_X$ of HCCI. Using multiple combustion modes, however, necessitates a strategy for switching between them. This paper presents a multi-mode combustion model and a simulation of a desirable transition from SI to HCCI.

There are several methods of achieving HCCI in internal combustion engines. For engines that use pre-mixed fuel and modest compression ratios, the pre-compression energy or fuel concentration of the cylinder contents must be raised so that the mixture will auto-ignite. Exhaust gases can be trapped by closing the exhaust valve early [1] or reinducted by closing the exhaust valve late [1,2], the intake can be heated or pre-compressed [3,4] or methods can be combined [5,6].

We achieve HCCI by reinducting hot exhaust gases along with fresh fuel and air (residual-affected HCCI). This form of HCCI eliminates the pumping losses associated with throttled SI [7,8]. The reinducted exhaust sinks heat during combustion, lowering the peak temperature and reducing $NO_X$. The exhaust also leaves less room for fresh reactants, reducing the work capacity of HCCI. SI can achieve more power and provide hot exhaust to initiate HCCI. It makes sense to include both modes in an engine.

In a multi-mode engine, mode transitions are necessary to vary work output smoothly through the space of engine capability. Martinez-Frias et al. suggest using SI with HCCI to reach higher loads [9]. Koopmans et al. have demonstrated mode transitions and have observed low work and advanced ignition phasing following a switch from SI to HCCI [10].
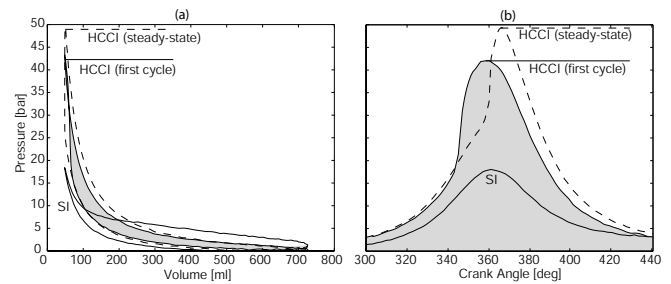


Figure 1. (a) P-V DIAGRAM OF AN EXPERIMENTAL SI TO HCCI MODE TRANSITION AND (b) PRESSURE TRACE ACROSS THE SAME TRANSITION

Switching from HCCI to SI is simple. SI combustion is predominantly independent of the previous cycle. Cooler cylinder wall temperatures after HCCI may slow the flame speed [10], but the switch to SI does not affect ignition timing. Switching to SI from HCCI is a fairly straightforward matter of choosing the transition points, switching to SI valve timings and turning on the spark.

Conversely, the SI to HCCI transition is complicated. When reinducted exhaust is used to induce HCCI, the intake and exhaust valves are open and unthrottled for much of the induction stroke. Hot products exhausted in the last combustion cycle are reinducted along with fresh reactants, raising the sensible energy of the mixture in the cylinder. The energy in the reinducted exhaust gas and quantity of fresh reactants dictate the point of ignition, work produced and exhaust temperature. Thus, the exhaust dynamically links cycles of residual-affected HCCI. The first cycle of HCCI combustion after a transition will depend on the exhaust temperature of SI combustion, complicating the transition.

Figure 1 provides evidence of the influence of SI exhaust on HCCI ignition. A transition from steady-state SI to steady-state HCCI valve timing exhibits early ignition on the first cycle following the transition. The total work for that cycle is much lower than steady state HCCI, Fig. 1 (a). Ignition phasing and engine work should be smooth regardless of the direction of the mode transition.

To explain the dynamics of the transition, the authors have created a multi-cycle, multi-mode model of SI and HCCI. The model uses several ordinary differential equations of state. Gas exchange, ignition and combustion are modeled to simulate SI and HCCI combustion. The exhaust manifold is modeled in order to capture cycle-to-cycle dynamics.

Based on cylinder pressure traces from simulation and experiment, the model correctly predicts premature HCCI phasing following an SI cycle. The model predicts that inducting less hot exhaust can retard the ignition to a nominal point. Simulation shows that closing the exhaust valve early to reduce exhaust reinduction can indeed correct the ignition phasing. However,

the lack of exhaust in the cylinder increases fresh reactant and work. To achieve the nominal work and ignition phasing, both exhaust and fresh reactant must be limited.

Exhaust temperature links HCCI to the previous combustion cycle, whether it be HCCI or SI. Relatively hot SI exhaust causes early, even pre-mature, ignition in the first cycle of HCCI following a mode transition. The multi-mode combustion model presented here captures this behavior. Simulation of the model with adjusted valve timing demonstrates an example trajectory that maintains constant work and ignition phasing. The model provides a tool for choosing valve timing to achieve a smooth transition.

## MODEL DESCRIPTION

The model is composed of several nonlinear ordinary differential equations of state. It is based on the first law of thermodynamics with:

- 1-D compressible flow through the intake and exhaust ports;
- Single-zone thermodynamic control-volume models of the cylinder and exhaust manifold;
- Heat transfer via simple convective models;
- Combustion via a Wiebe function; and,
- Ignition initiated by spark timing (SI) or an integrated Arrhenius threshold (HCCI).

It includes the following seven states:

1. Fuel concentration (kmol/m$^3$), $[fuel]$;
2. Oxygen concentration (kmol/m$^3$), $[O_2]$;
3. Nitrogen concentration (kmol/m$^3$), $[N_2]$;
4. Carbon dioxide concentration (kmol/m$^3$), $[CO_2]$;
5. Water concentration (kmol/m$^3$), $[H_2O]$;
6. Cylinder gas temperature (K), $T_c$; and,
7. Exhaust manifold internal energy (kJ/kg), $u_e$.

The model presented here is an extension of previous work and some details are left to the earlier treatment [11]. The model will be discussed in the following sections as the cylinder gas exchange, the combustion chamber control volume, and the exhaust manifold control volume.

## Gas Exchange

As in the physical system, valve timing dictates the flow into and out of the cylinder. Fresh products flow into the cylinder, $\dot{m}_{ic}$, when the intake valve is open. Similarly, exhaust flows from the cylinder to the exhaust manifold, $\dot{m}_{ce}$, or vice versa, $\dot{m}_{ec}$, when the exhaust valve is open. The valve strategy investigated here does not have significant flow from the cylinder back to the intake, so, these flows are not included. Figure 2 represents the flows visually.
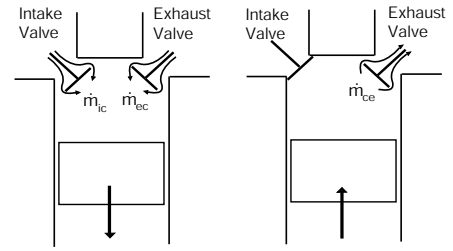


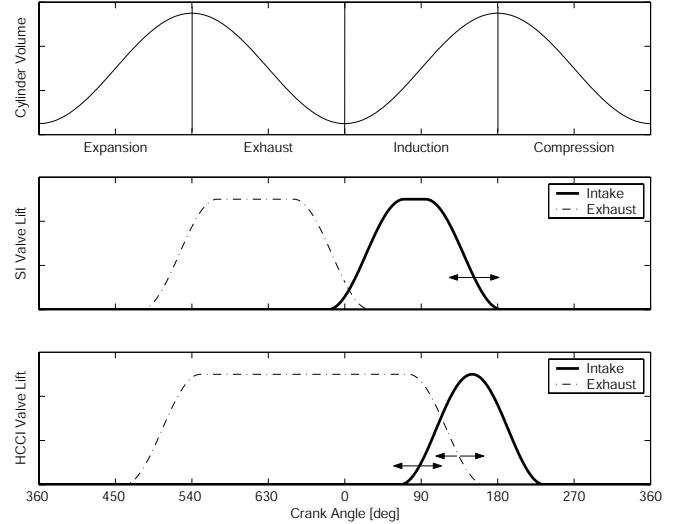Figure 2.    MASS FLOWS FOR INDUCTION AND EXHAUST



Figure 3.    TYPICAL VALVE PROFILES FOR SI AND HCCI

The valve profiles are quite different for SI and HCCI. During SI, the intake valve closing time is varied to adjust work. To reinduct exhaust for HCCI, the intake valve is opened later and the exhaust valve is held open for part of the induction stroke. Figure 3 shows typical valve profiles for SI and HCCI.

Gas flow into and out of the cylinder is described by one dimensional, steady-state, compressible, isentropic flow relations. The valve throttling is modeled by a discharge coefficient, $C_D$. Two general equations, Eqn. 1, are used for normal or choked flow, where $p_0$ is the pressure upstream of the valve and $p_T$ is the pressure downstream of the valve. The variables $p_T$, $p_0$, $T_0$, $A_R$ and $R$ in Eqn. 1 are replaced according to Tab. 1.

$$
\dot{m} = \begin{cases} \frac{C_D A_R p_0}{\sqrt{RT_0}} \left(\frac{p_T}{p_0}\right)^{\frac{1}{\gamma}} \sqrt{\frac{2\gamma}{\gamma-1}\left(1 - \left(\frac{p_T}{p_0}\right)^{\frac{\gamma-1}{\gamma}}\right)} & : \frac{p_T}{p_0} > \left(\frac{2}{\gamma+1}\right)^{\frac{\gamma}{\gamma-1}} \\[3mm] \frac{C_D A_R p_0}{\sqrt{RT_0}} \sqrt{\gamma\left(\frac{2}{\gamma+1}\right)^{\frac{\gamma+1}{\gamma-1}}} & : \frac{p_T}{p_0} \leq \left(\frac{2}{\gamma+1}\right)^{\frac{\gamma}{\gamma-1}} \end{cases}
\tag{1}
$$

Table 1. PARAMETERS FOR CALCULATING FLOW WITH EQN. (1)

|  | $p_T$ | $p_0$ | $T_0$ | $A_R$ | $R$ |
|---|---|---|---|---|---|
| $\dot{m}_{ic}$ | $p_c$ | $p_i = p_a$ | $T_i$ | $A_{iv}$ | $R_i$ |
| $\dot{m}_{ce}$ | $p_e = p_a$ | $p_c$ | $T_c$ | $A_{ev}$ | $R_c$ |
| $\dot{m}_{ec}$ | $p_c$ | $p_e = p_a$ | $T_e$ | $A_{ev}$ | $R_e$ |

## Combustion Chamber

The combustion chamber is modeled by a single control volume obeying the first law of thermodynamics.

$$\frac{d(m_c u_c)}{dt} = \dot{Q}_c - \dot{W}_c + \dot{m}_{ic} h_i - \dot{m}_{ce} h_c + \dot{m}_{ec} h_e \quad (2)$$

Heat transfer in the cylinder is modeled as pure convection with the cylinder wall in Eqn. 3. The convection coefficient, Eqns. 4-7, is modified from the Woschni equation in Stone [12]. The form and values are duplicated except for the convection coefficient scalar, $C_1$, which is modified for SI.

$$\dot{Q}_c = -\bar{h}_c A_c (T_c - T_{wall}) \quad (3)$$

$$\bar{h}_c = \frac{C_1 \left(C_2 \bar{v}_p p_c + C_3 \frac{p_c V_s T_{ign}}{p_{ign} V_{ign}} (p_c - p_a)\right)^{0.8}}{B_c^{0.2} T_c^{0.55}} \quad \frac{W}{m^2 K} \quad (4)$$

$$C_1 = \begin{cases} 259.6 : \text{SI} \\ 129.8 : \text{HCCI} \end{cases} \quad (5)$$

$$C_2 = \begin{cases} 6.18 : \text{gas exchange} \\ 2.28 : \text{otherwise} \end{cases} \quad (6)$$

$$C_3 = \begin{cases} 3.24 \times 10^{-3} : \text{combustion or expansion} \\ 0 \quad : \text{otherwise} \end{cases} \quad (7)$$

To calculate concentrations, the effect of combustion must be modeled. Combustion, modeled by a Wiebe function, immediately follows ignition. Spark ignition is simply modeled so that ignition occurs at the time spark is commanded, $\theta_{spark}$. HCCI ignition is modeled by the global Arrhenius rate integral.

$$\Psi = \int_{IVO}^{\theta} \frac{1}{\omega} A_k T_c^{n_k} e^{\frac{E_k}{RT}} [fuel]^{a_k} [O_2]^{b_k} d\theta \quad (8)$$

Ignition occurs when the integral, $\Psi$, passes a threshold, $\Psi_{th}$. Combustion continues until the fuel is fully consumed. Fuel is burned from $\Psi \geq \Psi_{th}$ in HCCI mode or $\theta \geq \theta_{spark}$ in SI mode until $N_{fuel} = 0$. The rate of fuel consumption is given by:

$$\dot{N}_{fuel} = \begin{cases} \dfrac{[fuel]_{ign} V_{ign} \omega \, a_W (m_W + 1) \left(\frac{\theta - \theta_{ign}}{\Delta\theta}\right)^{m_W}}{V_c \Delta\theta \, e^{a_W \left(\frac{\theta - \theta_{ign}}{\Delta\theta}\right)^{m_W + 1}}} : \text{combustion} \\ \\ 0 \qquad\qquad : \text{otherwise} \end{cases} \quad (9)$$

where, $\Delta\theta$ is the combustion duration.

The combustion duration is different for SI and HCCI and varies according to spark timing. Based on the empirical data, the duration of SI combustion is shorter for more advanced spark, Eqn. 10.

$$\Delta\theta = \begin{cases} \Delta\theta_{\text{HCCI}} \qquad : \text{HCCI} \\ \Delta\theta_{\text{SI}_{\text{offset}}} + \Delta\theta_{\text{SI}_{\text{slope}}} \theta_{\text{SI}} : \text{SI, where } \Delta\theta_{\text{SI}_{\text{slope}}} > 0 \end{cases} \quad (10)$$

While HCCI does exhibit changes in combustion duration, the total duration is so short that this effect is not included in the model.

Species consumption and production rates are scaled by the global reaction equation and the fuel consumption rate, $\dot{N}_{fuel}$. As an example, the global reaction presented here, Eqn. 11, is specifically for propane. The simulation is compared to experiments on propane, but the model can be parameterized for other fuels.

$$\phi C_3 H_8 + 5 O_2 + 18.8 N_2 \rightarrow$$
$$3\phi CO_2 + 4\phi H_2 O + 5(1 - \phi) O_2 + 18.8 N_2 \quad (11)$$
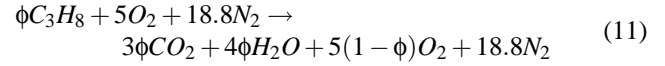
With equations for the mass flow and reaction, the concentration rates can be calculated. The rate of concentration change for species $j$, $[\dot{X}_j]$, is related, term-by term, to the flow into the cylinder, flow out of the cylinder, volume change and combustion reaction by:

$$[\dot{X}_j] = \frac{Y_{i,j} \dot{m}_{ic} + Y_{e,j} \dot{m}_{ec}}{V_c M_j} - \frac{[X_j] \dot{m}_{ce}}{\sum V_c [X_j] M_j} + \frac{\dot{V}_c N_j}{V_c^2} + \frac{\dot{N}_{rxn,j}}{V_c} \quad (12)$$

where,

- The mass fraction of gas in the intake, $Y_i$, corresponds to fresh reactants per the left side of Eqn. 11;
- The mass fraction of gas in the exhaust, $Y_e$, corresponds to completely burned products per the right side of Eqn. 11; and,
- The cylinder volume, $V_c$, and rate of volume change, $\dot{V}_c$, are based on the well known slider-crank relationship [12].
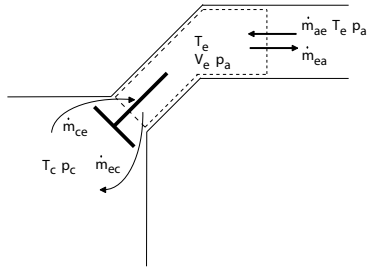
4

Figure 4. EXHAUST MANIFOLD CONTROL VOLUME AND MASS FLUX

Finally, given $\delta W = p\delta V$ and assuming ideal gas thermodynamic properties for pressure and energy, Eqn. 2 can be rearranged into a state equation for temperature, Eqn. 13.

$$\dot{T}_c = \frac{\left[ \begin{array}{c} \dot{Q}_c + \dot{m}_{ic}h_i + \dot{m}_{ec}h_e - \dot{m}_{ce}h_c - \\ \sum \left( V_c[\dot{X}_j]\hat{h}_{c,j} + \dot{V}_c[X_j]\hat{h}_{c,j} - \hat{R}T_cV_c[\dot{X}_j] \right) \end{array} \right]}{\sum V_c \left( T_c[X_j]\hat{c}_{p,j} - \hat{R}[X_j] \right)} \quad (13)$$

## Exhaust Manifold

Like the cylinder, the exhaust manifold is modeled as a control volume. One area of mass flux is the exhaust valve. The other is a fixed virtual edge. The exhaust manifold is represented visually in Fig. 4.

Flow through the exhaust valve, $\dot{m}_{ce}$ and $\dot{m}_{ec}$, is calculated with Eqn. 1. Flow through the virtual edge of the control volume, $\dot{m}_{ea}$ and $\dot{m}_{ae}$, occurs according to Eqn. 14 to maintain atmospheric pressure in the manifold at the temperature corresponding to the energy state, $u_e$.

$$\dot{m}_e = \dot{m}_{ce} - \dot{m}_{ec} + \dot{m}_{ae} - \dot{m}_{ea} \quad (14)$$

As in the cylinder model, the exhaust manifold model begins with the first law of thermodynamics, Eqn. 15.

$$\frac{d(m_eu_e)}{dt} = \dot{Q}_e - \dot{W}_e + \dot{m}_{ce}h_c - \dot{m}_{ec}h_e \quad (15)$$

Heat transfer is modeled as pure convection with a constant convection coefficient. There is no work since the size of the control volume is fixed.

$$\dot{Q}_e = \bar{h}_eA_e(T_a - T_e) \qquad \delta W_e = p_a\delta V_e = 0 \quad (16)$$

Using ideal gas relationships between specific heat and temperature, Eqns. 14, 15 and 16 can be combined into an equation for
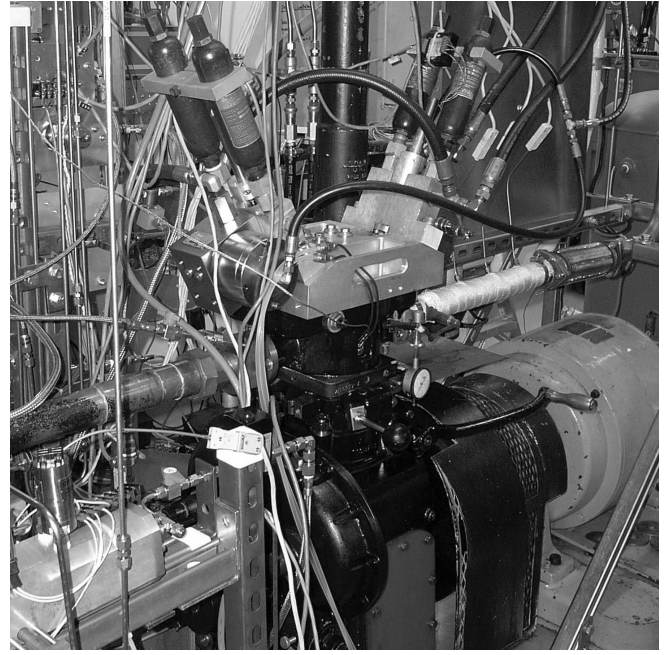


Figure 5. RESEARCH ENGINE WITH VARIABLE VALVE ACTUATION SYSTEM

the internal energy state.

$$\dot{u}_e = \frac{R_eT_e}{p_aV_e\gamma} \left( \dot{m}_{ce}(h_c - h_e) + \bar{h}_eA_e(T_a - T_e) \right) \quad (17)$$

Equations 12, 13 and 17 complete the state equations for the model.

## EXPERIMENTAL SETUP

A single cylinder research engine at Stanford provides data to validate the model. A closed-loop hydraulic variable valve actuation (VVA) system controls the valve timing with full timing control over both the intake and exhaust valves [13]. Figure 5 shows the engine and VVA. For SI, advancing IVC reduces the amount of mass inducted and thereby reduces engine work. IVO and EVC adjust the combustion phasing and work during HCCI.

Work estimates for experiments are based on 5 kHz in-cylinder pressure measurements and calculations of cylinder volume from engine position measured by a 4096 increment encoder. A fixed engine speed of 1800 revolutions per minute yields roughly 2 crank angle degrees between each sample. A relief valve controls high pressure propane so that fuel flow through a choked-flow orifice is slightly lean of stochiometry (0.95 equivalence ratio).
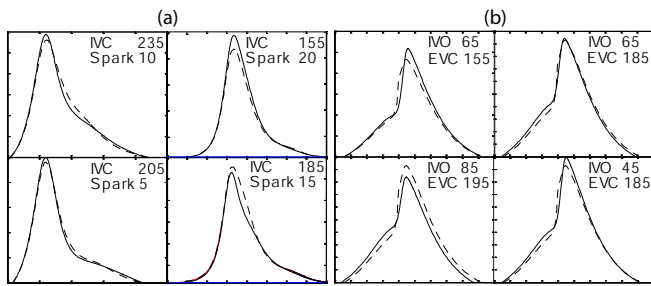
5

Figure 6. STEADY STATE (a) SI AND (b) HCCI CYLINDER PRESSURE TRACES FOR SIMULATION (SOLID) AND EXPERIMENT(DASHED)
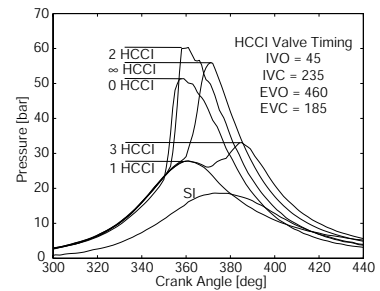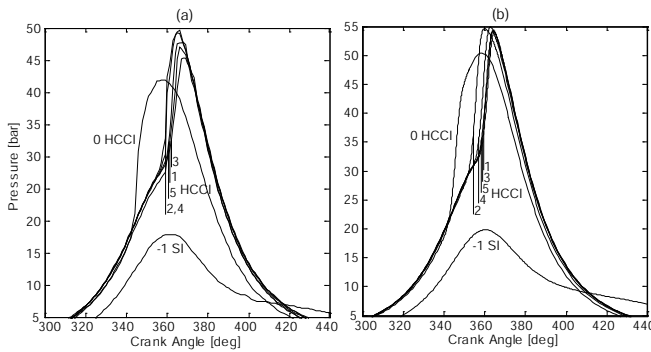


Figure 7. COMPARISON OF (a) MEASURED AND (b) SIMULATED CYLINDER PRESSURE TRACES DURING AN SI TO HCCI TRANSITION

## MODEL VALIDATION

Comparison of cylinder pressure traces demonstrates model accuracy. Steady-state cylinder pressure traces are shown in Fig. 6. For SI, there are four plots with different IVC and spark advance. For HCCI, there are also four plots. The IVO and EVC are different in each plot. The simulated peak pressure phasing, a proxy for ignition phasing, lines up with the measurement. The shape of the simulated pressure traces match experiment; slight magnitude errors indicate imperfect model parameterization.

The quality of the model depends heavily on the ability of the model to capture the effect of exhaust reinduction. The exhaust manifold model should predict transient HCCI behavior. Figure 7 shows experimental and simulated cylinder pressure traces over a transition from SI to HCCI. Again, the shape of the cylinder pressure traces and ignition phasing match remarkably well even if the traces do not align perfectly. The difference in scale is used to show the similarity in shape. The model correctly predicts early ignition and captures the dynamic effect of exhaust temperature.



Figure 8. EXPERIMENTAL SI TO HCCI MODE TRANSITION RESULTING IN A MISFIRE

## TRANSITION STRATEGY

Power and ignition phasing should be smooth across the mode transition. Figure 1 shows an uncontrolled transition from SI to HCCI at operating points with the same average IMEP. The first cycle of HCCI produces less work than the steady-state value. Hot SI exhaust leads to a hotter initial mixture of exhaust products and fresh reactants. This mixture is less dense than the nominal mixture so there is less fresh reactant as well as less reinducted exhaust. The higher initial temperature also advances auto-ignition. The basis for this is explained in the Arrhenius integral model of ignition, Eqn. 8. The temperature of the mixture is taken to a positive exponent, so higher intital temperatures will ignite earlier. Early ignition increases heat transfer losses, decreasing the energy available to perform work. Besides reducing the work, early ignition can have a whiplash effect. Figure 8 shows an experiment where early ignition caused the next cycle to misfire. Heat transfer losses coupled with less initial chemical energy serve to decrease engine work and destabilize HCCI combustion following transition from SI.

Early ignition on the first cycle indicates too much initial energy. The simulated SI exhaust temperature at the end of the exhaust stroke is 801°C compared to a steady state HCCI temperature of 381°C. Less of the hot exhaust is needed. Closing the exhaust valve earlier is one way to reduce the amount of exhaust inducted. Figure 9 (a) shows a simulation with early EVC. Iteratively chosen early EVC delays ignition to the nominal time. Despite similar compression work, the peak pressure is significantly higher, Fig. 9 (a). Work for this cycle is above nominal. When the exhaust valve is closed early, more fresh reactant is drawn into the cylinder leading to more chemical energy and thus more work.

To match nominal ignition phasing and work, exhaust and fresh reactant induction must both be restricted. There are several ways to restrict induction through either valve. Early IVC and EVC are used here. Figure 9 (b) shows the first cycle of HCCI with phasing and IMEP matching the steady state value. However, simulated exhaust temperature after the exhaust stroke of the first HCCI cycle, 549°C, is still higher than the steady state
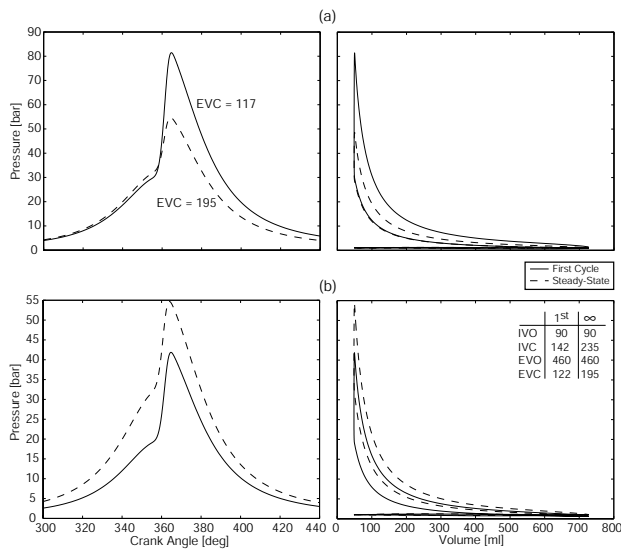
6

Figure 9. SIMULATION OF (a) FIRST HCCI CYCLE WITH EARLY EVC (b) FIRST HCCI CYCLE WITH EARLY IVC AND EVC (IMEP IS THE SAME AS STEADY STATE)

Table 2. SMOOTH TRANSITION SIMULATION PARAMETERS

|  | IVC [deg] | EVC [deg] | IMEP [bar] | Peak [deg] | $T_e$ [°C] |
|---|---|---|---|---|---|
| SI |  |  | 266 |  | 801 |
| HCCI 0 | 142 | 123 | 269 | 364.9 | 549 |
| HCCI 1 | 160 | 152 | 268 | 363.8 | 466 |
| HCCI 2 | 169 | 166 | 269 | 364.3 | 431 |
| HCCI 3 | 186 | 184 | 268 | 363.1 | 406 |
| HCCI 4 | 195 | 192 | 271 | 363.9 | 394 |
| HCCI 5 | 235 | 195 | 265 | 364.1 | 384 |
| HCCI ∞ | 235 | 195 | 269 | 364.8 | 381 |

temperature, 381°C.

The same technique can be employed on subsequent cycles to control ignition phasing and work. Table 2 shows the valve timings for a trajectory that achieved fairly constant ignition phasing and work. The IMEP from compression and expansion, phase of peak pressure, and exhaust temperature at the end of the exhaust stroke are also included. The pressure traces for the first few cycles are shown in Fig. 10.

Insight from the model reveals which transitions are feasible. HCCI needs to reinduct hot exhaust gases to auto-ignite. The consistently hotter gases associated with SI (relative to HCCI)
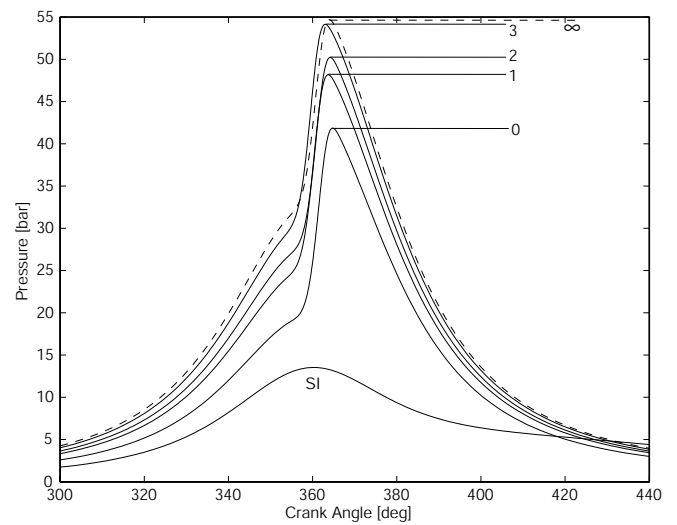


Figure 10. SI TO HCCI TRANSITION SIMULATION WITH CONSTANT WORK AND IGNITION PHASING

add more energy to the cylinder charge on a per-unit mass basis. However, the lower density of the hot gas will lead to less total mass being reinducted. From Eqn. 1, the mass flow is reduced by the square root of temperature. However, energy per unit mass increases roughly linearly with temperature. Since SI exhaust is hotter than HCCI exhaust, adequate internal energy can always be drawn into the cylinder from SI exhaust to ignite HCCI. As observed earlier, less exhaust is needed so adequate fresh reactants can always be inducted. So, hotter reinducted SI exhaust can ignite HCCI combustion at the nominal power and ignition phase of any self-sustainable HCCI operating condition.

## CONCLUSIONS

A multi-mode engine supporting SI and HCCI would offer the performance of popular SI engines with the emissions and efficiency benefits of HCCI. However, the exhaust dependence of residual-affected HCCI complicates the transition from SI. Specifically, hot SI exhaust advances ignition in the first cycle of HCCI and reduces the work produced. Both intake and exhaust induction must be restricted to achieve the desired ignition phasing and work.

A model has been presented that describes SI and HCCI combustion. Simulation of the model demonstrates a trajectory that achieves constant ignition phasing and work. This example exploits higher exhaust temperatures to achieve the appropriate initial cylinder sensible energy while restricting the total mass inducted. The model provides a tool to choose valve timings that achieve a smooth transition from SI to HCCI.

7

Copyright © 2004 by ASME

## FUTURE WORK

Scheduling every transition by the method used in the example in this paper would be difficult. In future work, the model will be used to develop a closed loop control scheme for ignition phase and work, as in [14], for HCCI after a transition.

## ACKNOWLEDGMENT

## REFERENCES

[1] Law, D., Kemp, D., Allen, J., Kirkpatrick, G., and Copland, T., 2001. "Controlled Combustion in an IC-engine with a fully variable valve train". *SAE paper 2001-01-0251* .

[2] Caton, P. A., Simon, A. J., Gerdes, J. C., and Edwards, C. F., 2003. "Residual-Effected Homogeneous Charge Compression Ignition at Low Compression Ratio Using Exhaust Reinduction". International Journal of Engine Research, **4** (2) , pp. 163–177.

[3] Tunestal, P., Olsson, J.-O., and Johansson, B., 2001. "HCCI Operation of a Multi-Cylinder Engine". *First Biennial Meeting of the Scandinavian-Nordic Section of the Combustion Institute* .

[4] Martinez-Frias, J., Aceves, S. M., Flowers, D., Smith, J. R., and Dibble, R., 2000. "HCCI Engine Control by thermal Management". *SAE paper 2000-01-2869* .

[5] Agrell, F., Angstrom, H.-E., Eriksson, B., Wikander, J., and Linderyd, J., 2003. "Integrated Simulation and Engine Test of Closed Loop HCCI Control by aid of Variable Valve Timings". *SAE paper 2003-01-0748* .

[6] Hyvönen, J., Haraldsson, G., and Johansson, B., 2003. "Supercharging HCCI to Extend the Operating Range in a Multi-Cylinder VCR-HCCI Engine". *SAE 2003-01-3214* .

[7] Najt, P. M., and Foster, D. E., 1983. "Compression-Ignited Homogeneous Charge Combustion". *SAE paper 830264* .

[8] Kaahaaina, N. B., Simon, A. J., Caton, P. A., and Edwards, C. F., 2001. "Use of Dynamic Valving to Achieve Residual-Affected Combustion". *SAE paper 2001-01-0549* .

[9] Martinez-Frias, J., Aceves, S. M., Flowers, D., Smith, J. R., and Dibble, R., 2003. "Equivalence Ratio-EGR Control of HCCI Engine Operation and the Potential for Transition to Spark-Ignited Operation". *SAE paper 2003-01-0753* .

[10] Koopmans, L., Strom, H., Lundgren, S., Backlund, O., and Denbratt, I., 2003. "Demonstrating a SI-HCCI-SI Mode Change on a Volvo 5-Cylinder Electronic Valve Control Engine". *SAE paper 2003-01-0753* .

[11] Shaver, G. M., Gerdes, J. C., Roelle, M. J., Caton, P. A., and Edwards, C. F., 2004. "Dynamic Modeling of Residual-Affected HCCI Engines with Variable Valve Actuation". *To appear at the ASME Journal of Dynamic Systems, Measurement and Control* .

[12] Stone, R., 1999. *Introduction to Internal Combustion Engines*. SAE International.

[13] Hathout, J.-P., Ahmed, J., and Kojic, A., 2004. "Reduced Order Modeling and Control of an Electrohydraulic Valve System". *First IFAC Symposium on Advances in Automotive Control* , pp. 182–187.

[14] Shaver, G. M., Gerdes, J. C., and Roelle, M. J., 2004. "Physics-Based Closed-Loop Control of Phasing, Peak Pressure and Work Output in HCCI Engines Utilizing Variable Valve Actuation". *Proceedings of the 2004 American Control Conference* , pp. 150–155.